THE JOURNAL OF BIOLOGICAL CHEMISTRY VOL. 286, NO. 46, pp. 40246–40254, November 18, 2011

The TREX1 Exonuclease R114H Mutation in Aicardi-Goutières Syndrome and Lupus Reveals Dimeric Structure Requirements for DNA Degradation Activity*◆

Received for publication, August 26, 2011, and in revised form, September 20, 2011 Published, JBC Papers in Press, September 21, 2011, DOI 10.1074/jbc.M111.297903

Clinton D. Orebaugh, Jason M. Fye, Scott Harvey, Thomas Hollis, and Fred W. Perrino[1]

From the Department of Biochemistry, Wake Forest School of Medicine, Winston-Salem, North Carolina 27157

Background: Mutations in the TREX1 exonuclease gene cause a spectrum of autoimmune diseases.
Results: The TREX1 Arg-114 residue acts across the stable dimer interface.
Conclusion: TREX1 residues in one protomer contribute to DNA degradation catalyzed in the opposing protomer.
Significance: These data help to explain the heterozygous disease condition.

Mutations in the *TREX1* gene cause Aicardi-Goutières syndrome (AGS) and are linked to the autoimmune disease systemic lupus erythematosus. The TREX1 protein is a dimeric 3′ DNA exonuclease that degrades DNA to prevent inappropriate immune activation. One of the most common TREX1 mutations, R114H, causes AGS as a homozygous and compound heterozygous mutation and is found as a heterozygous mutation in systemic lupus erythematosus. The TREX1 proteins containing R114H and the insertion mutations aspartate at position 201 (D201ins) and alanine at position 124 (A124ins), found in compound heterozygous AGS with R114H, were prepared and the DNA degradation activities were tested. The homodimer $TREX1^{R114H/R114H}$ exhibits a 23-fold reduced single-stranded DNA (ssDNA) exonuclease activity relative to $TREX1^{WT}$. The $TREX1^{D201ins/D201ins}$ and $TREX1^{A124ins/A124ins}$ exhibit more than 10,000-fold reduced ssDNA degradation activities. However, the $TREX1^{R114H/D201ins}$ and $TREX1^{R114H/A124ins}$ compound heterodimers exhibit activities 10-fold greater than the $TREX1^{R114H/R114H}$ homodimer during ssDNA and double-stranded DNA (dsDNA) degradation. These higher levels of activities measured in the $TREX1^{R114H/D201ins}$ and $TREX1^{R114H/A124ins}$ compound heterodimers are attributed to Arg-114 residues of $TREX1^{D201ins}$ and $TREX1^{A124ins}$ positioned at the dimer interface contributing to the active sites of the opposing $TREX1^{R114H}$ protomer. This interpretation is further supported by exonuclease activities measured for TREX1 enzymes containing R114A and R114K mutations. These biochemical data provide direct evidence for TREX1 residues in one protomer contributing to DNA degradation catalyzed in the opposing protomer and help to explain the dimeric TREX1 structure required for full catalytic competency.

Nucleases process DNA and RNA to prevent inappropriate immune activation. TREX1 is the most abundant 3′→5′ exonuclease detected in mammalian cells and degrades both ssDNA[2] and dsDNA (1–4). Deletion of the *TREX1* gene in mice elicits an interferon-dependent autoimmune phenotype characterized by inflammatory myocarditis and a dramatically shortened lifespan (5–7). More than 40 mutations in human *TREX1* are linked to a spectrum of autoimmune disorders including Aicardi-Goutières syndrome (AGS) (8, 9), familial chilblain lupus (10, 11), retinal vasculopathy with cerebral leukodystrophy (12), and systemic lupus erythematosus (SLE) (13, 14). These autoimmune disorders show clinical overlap with findings of raised type-I interferon, cerebrospinal fluid lymphocytosis, circulating antibodies to ssDNA and dsDNA, lupus-like rash, and progressive encephalopathy with intracranial calcifications (9, 15–18). Thus, persistent DNA resulting from the dysfunctional TREX1 enzyme activates the immune system leading to autoimmunity.

The *TREX1* gene encodes a 314-amino acid protein. The TREX1 N-terminal 242 amino acids contain the catalytic domain and the C-terminal region contains a proposed transmembrane helix that is not found in TREX2. TREX1 and TREX2 have similar homodimeric structures with distinct elements that point to different biological roles (19, 20). Deletion of the *TREX2* gene in mice increases susceptibility to induced skin carcinogenesis (21), contrasting the autoimmune phenotype of the *TREX1* knock-out mouse. The TREX1 dimer has an 8-amino acid polyproline II helix on the top and bottom of the front face and the TREX2 dimer has a β-hairpin in the same position. The TREX1 enzyme has a flexible region positioned adjacent to the active site that has a sequence distinct from the DNA binding loop adjacent to the TREX2 active site. The TREX1 C-terminal region localizes the enzyme to the endoplasmic reticulum in the perinuclear space of cells (6, 12, 22). TREX1 relocates to the nucleus upon activation of a cell death pathway or by treatment of cells with DNA-damaging agents (7, 22) where it presumably acts to degrade DNA.

The TREX1 dimeric structure is maintained by an extensive interface that involves 1650 Å^2 of buried surface area from each monomer, equivalent to 15% of the monomer surface (20). The

* This work was supported, in whole or in part, by National Institutes of Health Grant GM069962 (to F. W. P.), Alliance for Lupus Research Grant 179222 (to F. W. P.), and American Heart Association Grant 10GRNT3650033 (to T. H.).
◆ This article was selected as a Paper of the Week.
[1] To whom correspondence should be addressed. Tel.: 336-716-4349; Fax: 336-716-7671; E-mail: fperrino@wfubmc.edu.

[2] The abbreviations used are: ssDNA, single-stranded DNA; AGS, Aicardi-Goutières syndrome; SLE, systemic lupus erythematosus; dsDNA, double-stranded DNA; MBP, maltose-binding protein.

hydrogen-bonding network between protomers includes backbone contacts of the β3 strands and six pairs of side chain contacts. The antiparallel α4 helices contribute hydrophobic packing interactions between the protomers. The dimeric structure of TREX1 is unusual for 3′→5′ exonucleases and contributes to the dominant autoimmune phenotype in some TREX1 mutations (23). The metal ion-binding residues Asp-18, Glu-20, Asp-130, and Asp-200 positions at the TREX1 active site, and the D18N, D200N, and D200H heterozygous mutations have been identified in dominant familial chilblain lupus and AGS (10, 11, 18, 24, 25). The TREX1 enzymes containing dominant D18N, D200N, and D200H mutations are defective in dsDNA degradation activity, and these TREX1 mutants inhibit the dsDNA degradation activity of the TREX1^{WT} enzyme explaining the dominant phenotypes of these *TREX1* mutant alleles (23, 26).

One of the most common *TREX1* mutations found in autoimmune disease is the single nucleotide Gua→Ade missense mutation at position 341 causing the R114H substitution. The *TREX1* R114H is found as homozygous and compound heterozygous in more than 60 AGS-associated disease genotypes (8, 9, 17) and R114H is mostly heterozygous in SLE with a single homozygous R114H SLE patient identified (13, 14). The TREX1 Arg-114 residue is about 15 Å removed from the active site positioned at the dimer interface where it hydrogen bonds with two backbone carbonyl oxygens of the opposing protomer. The TREX1$^{R114H/R114H}$ homodimer exhibits severely reduced enzymatic activity on ss- and dsDNA compared with TREX1^{WT} (20, 23).

Compound heterozygote individuals carrying the *TREX1* R114H and D201ins alleles or the *TREX1* R114H and A124ins alleles have been identified in AGS (8). The *TREX1* D201ins mutation is caused by a three-nucleotide GAT insertion mutation between nucleotides 600 and 601 resulting in the insertion of an extra aspartate at amino acid position 201. The *TREX1* A124ins mutation is caused by a three-nucleotide GGC insertion mutation between nucleotides 368 and 369 resulting in the insertion of an extra alanine at position 124.

The mechanism by which R114H causes TREX1 catalytic dysfunction was determined. The considerable distance of Arg-114 from the TREX1 catalytic center and its location at the dimer interface raised the possibility that this residue affects activity in the opposing protomer of the TREX1 dimer. The TREX1$^{R114H/D201ins}$ and TREX1$^{R114H/A124ins}$ compound heterodimers were prepared and the remarkable stability of the TREX1 dimer was demonstrated. The activities of TREX1 R114H-containing homodimers, heterodimers, and compound heterodimers were compared with TREX1^{WT} using quantitative ss- and dsDNA degradation assays. The activities measured in these TREX1 R114H mutants demonstrate that Arg-114 from one TREX1 protomer participates in DNA degradation occurring in the opposing protomer. This conclusion is further substantiated in TREX1 mutant homodimers, heterodimers, and compound heterodimers containing R114A and R114K. These data help to explain the stable TREX1 dimeric structure necessary for biological function and support the observed autoimmune phenotypes.

EXPERIMENTAL PROCEDURES

Materials—The synthetic 30-mer oligonucleotide 5′-ATACGACGGTGACAGTGTTGTCAGACAGGT-3′ with 5′ fluorescein was from Eurofins. Plasmid 1 (9.4 kb) was nicked with the Nt.BbvCI restriction endonuclease as previously described (23).

Enzyme Preparation—The human TREX1^{WT} and mutant homo- and heterodimer enzymes were prepared as previously described (20, 23). Briefly, mutant *TREX1*-containing plasmids were produced using a PCR site-directed mutagenesis strategy (27) and confirmed by DNA sequencing. The TREX1^{WT} and mutant homodimer enzymes (amino acids 1–242) were produced in bacteria as N-terminal maltose-binding protein (MBP) fusions with a PreScission Protease recognition sequence between the MBP and TREX1. The MBP-TREX1 fusion protein was bound to an amylose resin (New England Biolabs), washed, and the TREX1 was separated from MBP with PreScission Protease (GE Biosciences). The TREX1 was collected and purified to homogeneity using phosphocellulose chromatography.

To generate TREX1 heterodimers, one *TREX1*-containing plasmid was engineered to express MBP-TREX1 and a second to express His-NusA-TREX1. The two plasmids were co-expressed in the same bacterial cell to generate a mixture of TREX1 homodimers containing only the MBP, only the His-NusA affinity tags, and TREX1 heterodimers containing both affinity tags. The TREX1 heterodimers were separated from the homodimers by sequential chromatography using nickel-nitrilotriacetic acid (Qiagen) and amylose resins (New England Biolabs). The TREX1 heterodimers were purified by phosphocellulose chromatography.

Several affinity-tagged TREX1 fusion proteins were prepared to perform dimer stability studies. The His-NusA-TREX1^{WT} homodimer was purified by nickel affinity and MonoQ chromatography. The His-MBP-TREX1^{WT} and His-MBP-TREX1^{R114H} homodimers were purified by nickel affinity chromatography and collected in the flow-through from a MonoQ column. The mixture of His-NusA-TREX1^{WT} homodimers with His-NusA-TREX1^{WT}/His-MBP-TREX1^{WT} heterodimers was generated by coexpression of the two affinity-tagged TREX1 fusion protein constructs and subsequent purification by nickel affinity and MonoQ chromatography. All protein concentrations were determined by A_{280} using molar extinction coefficients for the TREX1 protomer, ϵ = 23,950 M^{-1} cm^{-1}; His-MBP-TREX1, ϵ = 90,300 M^{-1} cm^{-1}; His-NusA-TREX1, ϵ = 54,890 M^{-1} cm^{-1}; and the His-NusA-TREX1, His-NusA-TREX1/His-MBP-TREX1 mixture, ϵ = 63,743 M^{-1} cm^{-1}.

Dimer Stability Assays—The TREX1 dimer stability assays (500 μl) contained 50 mM Tris (pH 7.5), 50 mM NaCl, 1 mM EDTA, 10% glycerol, and the indicated amounts of TREX1^{WT} or variant and His-MBP-TREX1^{WT} or His-MBP-TREX1^{R114H}. The reactions were incubated as described in the legend of Fig. 2. Amylose resin (30 μl) was added to the reaction and incubated with rotation for 60 min at 4 °C. The resin was washed with 1 ml of buffer A (20 mM Tris, pH 7.5, 200 mM NaCl, 1 mM EDTA) three times and the bound proteins were eluted with

200 μl of buffer A containing 20 mM maltose. Samples of the eluted proteins were analyzed by SDS-PAGE and gels were stained with Coomassie Blue (Bio-Rad).

Exonuclease Assays—The exonuclease assays contained 20 mM Tris (pH 7.5), 5 mM $MgCl_2$, 2 mM dithiothreitol, 100 μg/ml of bovine serum albumin, 50 nM fluorescein-labeled 30-mer oligonucleotide (ssDNA assay) or 10 μg/ml of nicked plasmid DNA (dsDNA assay), and TREX1 protein as indicated in the legends of Figs. 3–6. Reactions were incubated at 25 °C for 15 min or as indicated, quenched by the addition of 3 volumes of cold ethanol, and dried *in vacuo*. For ssDNA assays, the reaction products were resuspended in 4 μl of formamide and separated on 23% denaturing polyacrylamide gels. Fluorescently labeled bands were visualized and quantified using a Storm PhosphorImager (GE Healthcare). The fraction of oligomer at each position was multiplied by the number of dNMPs excised from the 30-mer and by the total femtomoles of 30-mer in the starting reaction to determine the activities for $TREX1^{WT}$ and variants (fmol dNMP/s/fmol Enzyme) (19, 20, 23, 26).

For visualization of dsDNA reaction products, assays were resuspended in 20 μl of TAE-agarose gel running solution and electrophoresed on 0.8% agarose gels containing ethidium bromide. DNA was visualized using a FluorChem 8900 imaging system (Alpha Innotech). Our dsDNA assay (23) was modified to precisely quantify the TREX1 dsDNA degradation using fluorescence emission. Samples (20 μl) were removed at the indicated times and quenched in wells of a 384-well plate containing 20 μl of 15× SYBR Green I dye (Invitrogen). Fluorescent emission at 520 nm was determined using a POLARstar Omega microplate reader (BMG LABTECH). The amount of dsDNA remaining was determined by comparing fluorescence values to those obtained from a standard curve of fluorescence emission using varied plasmid 1 concentrations (0.1–15 μg/ml) stained with SYBR Green. The amount of dsDNA degraded was used to calculate dNMPs excised and activities for $TREX1^{WT}$ and variants (femtomole of dNMP/s/fmol of enzyme).

RESULTS AND DISCUSSION

A series of TREX1 R114H-containing mutants was prepared to test the hypothesis that the Arg-114 residue of one protomer positioned at the dimer interface contributes to the catalytic function of the opposing protomer within a TREX1 dimer. Gel filtration analysis of TREX1 purified as an endogenous protein from mammalian cells (1, 28) and as a recombinant enzyme expressed in bacterial cells (3) indicate a native molecular mass consistent with a dimer structure. There is no evidence of a TREX1 protein as a monomer in these enzyme preparations. The TREX1 structure confirms the dimeric nature of the exonuclease (20). TREX1 protomers form a dimer through extensive interactions between the β3 strands of the central β-sheet and the α4 helices of each protomer (Fig. 1). The Arg-114 residues are about 15 Å away from their respective active sites positioned at opposite edges of the dimer interface. This considerable distance from the catalytic center raises questions about how mutation of Arg-114 to histidine causes reduced ss- and dsDNA degradation activities in the $TREX1^{R114H/R114H}$ homodimer (20, 23). The TREX1 dimer 2-fold axis of symmetry positions the active sites on opposite edges of the same face.

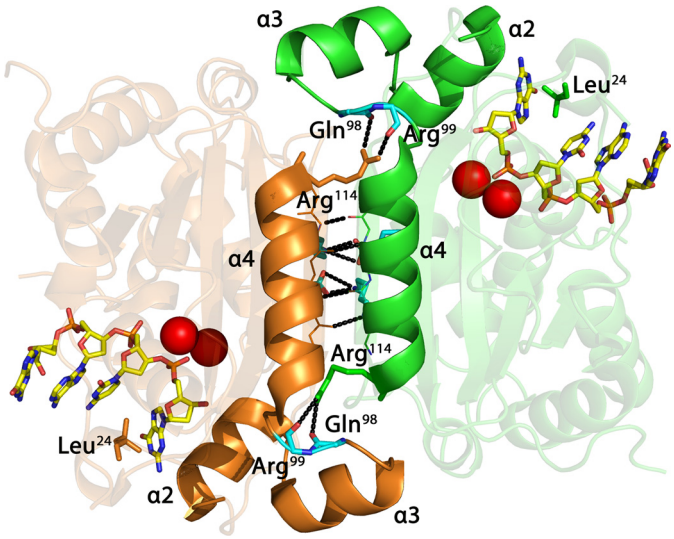

FIGURE 1. **The TREX1 dimer with bound ssDNA.** The interface between TREX1 protomers (*orange* and *green*) at the α4 helices and β3 strands is shown. Arg-114 residues (*orange* and *green*) extend from the ends of the α4 helices and form hydrogen bonds with the backbone carbonyl oxygens of Gln-98 and Arg-99 (*cyan*) positioned on a loop between the α3 and α4 helices of the opposing protomer. The nitrogenous base of the 3′ ssDNA nucleotide interacts with the hydrophobic face of the α2 helix and Leu-24 to maintain proper positioning for catalysis. Hydrogen bonding (*black dotted lines*) at the dimer interface is indicated. The metal ions (*red spheres*) and 4-mer ssDNA (as *sticks*) are shown bound in the active sites. The figure was prepared using PyMol (Schrodinger, LLC).

The 3′ nucleotide base of the DNA substrate is stabilized in a hydrophobic pocket between Leu-24 and the hydrophobic face of helix α2. The helix-loop-helix motifs formed by helices α2 and α3 are positioned on opposite edges at the dimer interface (Fig. 1). The Arg-114 side chain extends from the α4 helix of one TREX1 protomer and hydrogen bonds with the backbone carbonyl oxygens of residues Gln-98 and Arg-99 positioned on a loop after the α3 helix in the opposing protomer. Mutation of Arg-114 to histidine could disrupt critical contacts between Arg-114 and the opposing protomer altering position of the α2 helix to perturb positioning of the 3′ terminal nucleotide for cleavage.

Stability of the TREX1 Dimer—TREX1 expressed as a recombinant enzyme in bacterial cells generates kinetically stable dimers that do not dissociate and re-equilibrate at measurable rates. An experimental strategy was developed to measure the stability of the TREX1 dimer (Fig. 2). Equimolar mixtures of His-MBP-$TREX1^{WT}$ and $TREX1^{WT}$ homodimers were incubated for up to 4 h at 4 and 25 °C. The MBP-tagged enzyme was recovered using amylose resin and visualized by SDS-PAGE in an attempt to provide evidence for dissociation and reassociation of TREX1 protomers originating from the different homodimer populations. The His-MBP-$TREX1^{WT}$ was recovered from the mixtures with no detectable $TREX1^{WT}$ protomer that would have been present in His-MBP-$TREX1^{WT}$/$TREX1^{WT}$ heterodimers generated during a dissociation and re-equilibration process (Fig. 2*A*, *lanes 2–5*). In a further attempt to detect TREX1 dimer re-equilibration, the concentration of $TREX1^{WT}$ was increased in the mixture to a 8-fold molar excess over the His-MBP-$TREX1^{WT}$ protein. The mixture was incubated for 16 h at 4 °C, and the His-MBP-

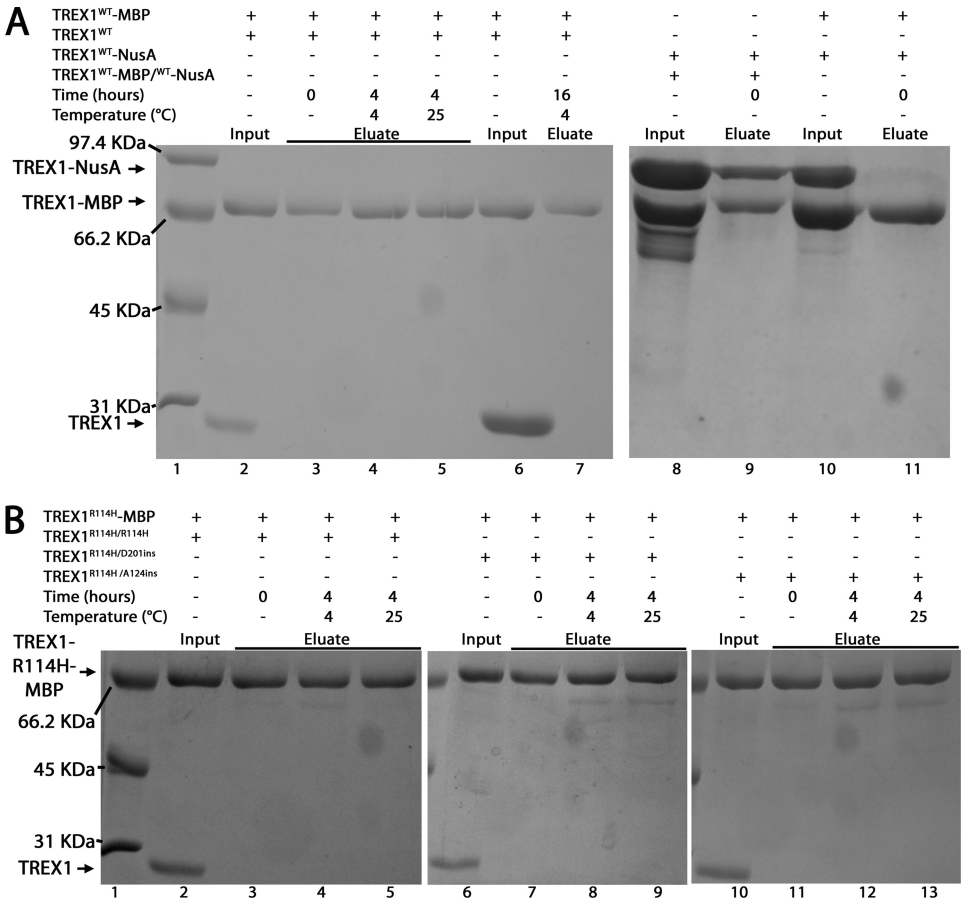

FIGURE 2. **Stability of the TREX1 dimer.** *A*, mixtures of TREX1^{WT} (2.5 μM, *lanes 2–5*, or 20 μM, *lanes 6* and *7*) and His-MBP-TREX1^{WT} (2.5 μM, *lanes 2–7*) were incubated as indicated. Also, a mixture of His-NusA-TREX1^{WT} homodimers with His-NusA-TREX1^{WT}/His-MBP-TREX1^{WT} heterodimers (2.5 μM, *lanes 8* and *9*) and a mixture of His-MBP-TREX1 homodimers (2.5 μM, *lanes 10* and *11*) and His-NusA-TREX1 homodimers (2.5 μM, *lanes 10* and *11*) were prepared. *B*, mixtures of TREX1$^{R114H/R114H}$ (2.5 μM, *lanes 2–5*), TREX1$^{R114H/D201ins}$ (2.5 μM, *lanes 6–9*), or TREX1$^{R114H/A124ins}$ (2.5 μM, *lanes 10–13*) and His-MBP-TREX1^{R114H} (2.5 μM, *lanes 2–13*) were incubated as indicated. The MBP-tagged protein was recovered as described under "Experimental Procedures." The input samples (*A*, *lanes 2, 6, 8*, and *10*; and *B*, *lanes 2, 6*, and *10*) and eluate samples (*A*, *lanes 3–5, 7, 9*, and *11*; and *B*, *lanes 3–5*, *7–9*, and *11–13*) were electrophoresed on 12% SDS-PAGE gels and stained with Coomassie Blue. *Lane 1* in *A* and *B* contain the indicated molecular weight standards.

TREX1^{WT} protein was again recovered with no evidence for the generation of His-MBP-TREX1^{WT}/TREX1^{WT} heterodimers (Fig. 2*A*, *lanes 6* and *7*). To demonstrate that stable TREX1 dimers are recovered using the amylose resin, the His-NusA-TREX1^{WT} protein present in the His-NusA-TREX1^{WT}/His-MBP-TREX1^{WT} heterodimer was recovered from a mixture of His-NusA-TREX1^{WT} homodimers and His-NusA-TREX1^{WT}/His-MBP-TREX1^{WT} heterodimers (Fig. 2*A*, *lanes 8* and *9*). This result contrasts with the recovery of only the His-MBP-TREX1^{WT} protein using the amylose resin from a mixture of His-NusA-TREX1^{WT} and His-MBP-TREX1^{WT} homodimers (Fig. 2*A*, *lanes 10* and *11*). These results demonstrate that the TREX1^{WT} protomers form stable dimers that do not dissociate and re-equilibrate at detectable levels under the conditions routinely used in our exonuclease activity assays.

The TREX1 R114H-containing mutants also form stable dimers. A series of TREX1 R114H mutant enzymes was prepared to determine whether mutation of Arg-114 positioned at the dimer interface affects TREX1 dimer stability. The His-MBP-TREX1^{R114H} homodimer was mixed with equimolar amounts of the TREX1^{R114H} homodimer (Fig. 2*B*, *lanes 2–5*), TREX1$^{R114H/D201ins}$ heterodimer (Fig. 2*B*, *lanes 6–9*), and TREX1$^{R114H/A124ins}$ heterodimer (Fig. 2*B*, *lanes 10–13*) and incubated for up to 4 h at 4 and 25 °C. The MBP-tagged enzyme was recovered using amylose resin and visualized by SDS-PAGE. The His-MBP-TREX1^{R114H} was recovered from the mixtures with no detectable untagged TREX1 protomer. Increased concentrations of untagged TREX1^{R114H} homodimer in the mixtures up to a 8-fold molar excess over the His-MBP-TREX1^{R114H} protein indicated no evidence for TREX1 dissociation and re-equilibration in the protein mixtures (data not shown). Thus, the TREX1 R114H mutation does not measurably effect the formation of stable TREX1 dimers.

The TREX1 3′ ssDNA Exonuclease Activities of Arg-114-containing Mutants—The *TREX1*$^{R114H/D201ins}$ compound heterozygous genotype has been identified in AGS (8). Because TREX1 is a stable dimer, cells of an individual with this genotype could contain TREX1$^{R114H/R114H}$ and TREX1$^{D201ins/D201ins}$ homodimers and TREX1$^{R114H/D201ins}$ heterodimers. The TREX1$^{R114H/R114H}$ and TREX1$^{D201ins/D201ins}$ homodimers exhibit about 23- and 19,000-fold reduced ssDNA exonuclease activities, respectively (Fig. 3), consistent with our previous studies (20, 23). The greatly reduced ssDNA exonuclease activity of the TREX1$^{D201ins/D201ins}$ homodimer is likely due to the aspartate insertion mutation acutely disrupting the α8-helix and preventing proper positioning of the catalytic residues for

A

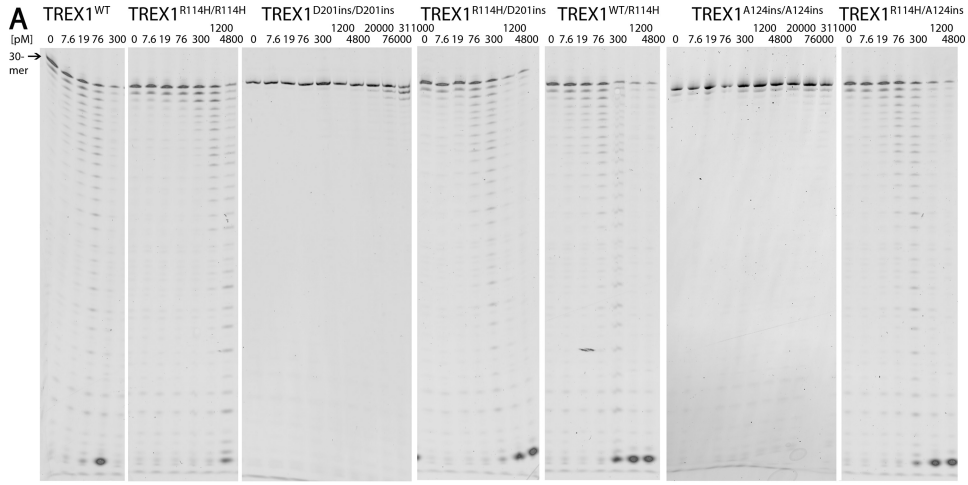

B

TREX1 Dimer	Activity (fmol/s/fmol E)	Relative Activity
TREX1^{WT}	6.3 ± 0.24	1
TREX1$^{R114H/R114H}$	0.28 ± 0.0071	1/23
TREX1$^{D201ins/D201ins}$	0.00034 ± 0.000036	1/19,000
TREX1$^{R114H/D201ins}$	2.9 ± 0.16	1/2.2
TREX1$^{WT/R114H}$	3.1 ± 0.12	1/2.0
TREX1$^{A124ins/A124ins}$	0.00016 ± 0.000012	1/39,000
TREX1$^{R114H/A124ins}$	2.6 ± 0.12	1/2.4

FIGURE 3. **The ssDNA exonuclease activities of TREX1^{WT}, R114H, D201ins, and A124ins variants.** *A*, standard exonuclease reactions were prepared with a fluorescein-labeled 30-mer oligonucleotide and dilutions of the recombinant TREX1^{WT}, TREX1$^{R114H/R114H}$, TREX1$^{D201ins/D201ins}$, TREX1$^{A124ins/A124ins}$, TREX1$^{WT/R114H}$, TREX1$^{R114H/D201ins}$, and TREX1$^{R114H/A124ins}$ were prepared at 10 times the final concentrations. Samples (3 μl) containing the TREX1 enzymes were added to reactions to yield the final indicated concentrations and reactions were incubated 15 min at 25 °C. The reaction products were subjected to electrophoresis on 23% urea-polyacrylamide gels and quantified as described under "Experimental Procedures." *B*, to precisely quantify results, the TREX1^{WT} and variant enzymes were assayed in triplicate at three different concentrations as described above. TREX1^{WT} was assayed at 8, 15, and 20 pM, TREX1$^{WT/R114H}$, TREX1$^{R114H/D201ins}$, and TREX1$^{R114H/A124ins}$ were assayed at 30, 45, and 60 pM, TREX1$^{R114H/R114H}$ was assayed at 150, 200, and 300 pM, and TREX1$^{D201ins/D201ins}$ and TREX1$^{A124ins/A124ins}$ were assayed at 1.5, 2.3, and 3 μM. Plots of activity *versus* enzyme concentrations were used to confirm the linearity of the assay and generate the enzyme activity values. The average activities and S.E. were determined by regression analysis using SigmaPlot 8.02 (SPSS Science, Inc.). The relative activity was calculated as: relative activity = 100 × ((femtomole of dNMP released/s/fmol of mutant enzyme)/(fmol of dNMP released/s/fmol of WT enzyme)). The position of migration of the 30-mer is indicated.

nucleotide hydrolysis (20). The TREX1$^{R114H/D201ins}$ heterodimer was prepared, and the ssDNA exonuclease activity was 2.2-fold reduced compared with TREX1^{WT} (Fig. 3). This modest reduction in activity indicates that the TREX1$^{R114H/D201ins}$ heterodimer is about 20-fold more active than predicted if each protomer in the heterodimer acted independently. The TREX1$^{R114H/D201ins}$ compound heterodimers would be expected to exhibit a 46-fold reduced 3′ exonuclease activity compared with TREX1^{WT}. Instead, this 20-fold higher activity measured in the TREX1$^{R114H/D201ins}$ heterodimer is attributed to Arg-114 of the TREX1^{D201ins} protomer contributing to ssDNA degradation in the TREX1^{R114H} protomer. Similarly, Arg-114 from the TREX1^{WT} protomer in the TREX1$^{WT/R114H}$ heterodimer contributes to activity in the TREX1^{R114H} protomer (Fig. 3), and the measured activities of the TREX1$^{R114H/D201ins}$ and TREX1$^{WT/R114H}$ heterodimers are attributed to the TREX1^{R114H} protomer active site. These data provide direct evidence for contributions of Arg-114 to ssDNA exonuclease activity across the dimer interface in the TREX1 dimer.

A compound heterozygous AGS individual with a *TREX1*$^{R114H/A124ins}$ genotype has also been identified.[3] The TREX1$^{A124ins/A124ins}$ homodimer and TREX1$^{R114H/A124ins}$ heterodimer exhibit about 39,000- and 2.4-fold reduced ssDNA exonuclease activities, respectively (Fig. 3). The additional Ala-124 insertion in the TREX1$^{A124ins/A124ins}$ homodimer likely alters positioning of the Arg-128 DNA-binding residue and the Asp-130 metal-binding residue resulting in a dramatic reduction in ssDNA degradation activity. Similar to the TREX1$^{R114H/D201ins}$ heterodimer, the TREX1$^{R114H/A124ins}$ heterodimer ssDNA degradation activity is about 20-fold more active than predicted based on the activities of the TREX1$^{A124ins/A124ins}$ and TREX1$^{R114H/R114H}$ homodimers, further supporting the concept that Arg-114 from the TREX1^{A124ins} protomer contributes to ssDNA exonuclease activity in the opposing TREX1^{R114H} protomer.

The TREX1$^{WT/R114H}$, TREX1$^{R114H/D201ins}$, and TREX1$^{R114H/A124ins}$ heterodimers have nearly identical ssDNA exonuclease activities that are reduced about 2-fold compared with TREX1^{WT} (Fig. 3). Replacing the TREX1^{WT} protomer with a TREX1^{D201ins} or TREX1^{A124ins} protomer does not further reduce the DNA degradation activity compared with the TREX1$^{WT/R114H}$ heterodimer. This is despite the nearly complete lack of catalytic potential in the Asp-201ins and Ala-124ins mutants apparent from the 10^4-fold reduced activities of the TREX1$^{D201ins/D201ins}$ and TREX1$^{A124ins/A124ins}$ homodimers. These data indicate that the TREX1^{R114H} protomer active site is responsible for the ssDNA exonuclease activities measured in these TREX1 R114H-containing het-

[3] Y. Crow, unpublished data.

A

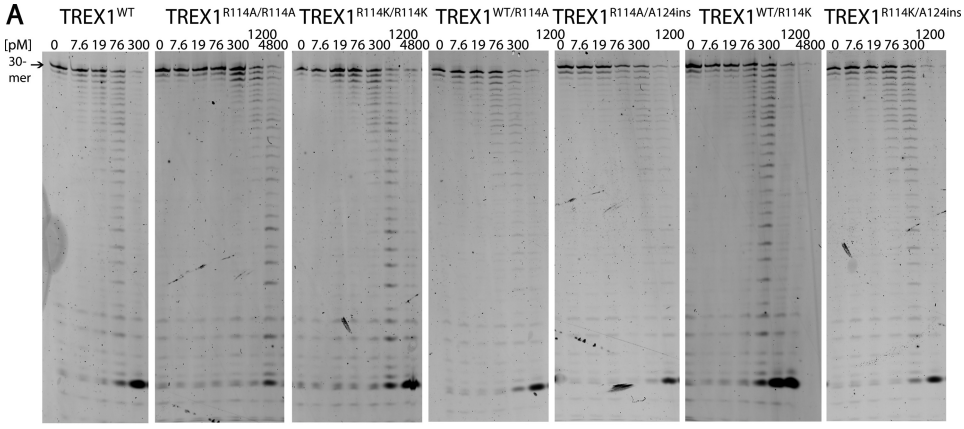

B

TREX1 dimer	Activity *(fmol/s/fmol E)*	Relative Activity
$TREX1^{WT}$	6.3 ± 0.24	1
$TREX1^{R114A/R114A}$	0.29 ± 0.015	1/22
$TREX1^{R114K/R114K}$	0.58 ± 0.017	1/11
$TREX1^{WT/R114A}$	1.6 ± 0.11	1/3.8
$TREX1^{R114A/A124ins}$	1.1 ± 0.087	1/5.8
$TREX1^{WT/R114K}$	2.5± 0.13	1/2.5
$TREX1^{R114K/A124ins}$	1.9 ± 0.11	1/3.2

FIGURE 4. **The ssDNA exonuclease activities of $TREX1^{WT}$, R114A, and R114K variants.** *A*, standard exonuclease reactions were prepared with a fluorescein-labeled 30-mer oligonucleotide and dilutions of the recombinant $TREX1^{WT}$, $TREX1^{R114A/R114A}$, $TREX1^{R114K/R114K}$, $TREX1^{WT/R114A}$, $TREX1^{WT/R114K}$, $TREX1^{A124ins/R114A}$, and $TREX1^{A124ins/R114K}$ were prepared at 10 times the final concentrations. Samples (3 μl) containing the TREX1 enzymes were added to reactions to yield the final indicated concentrations and reactions were incubated 15 min at 25 °C. The reaction products were subjected to electrophoresis on 23% urea-polyacrylamide gels and quantified as described under "Experimental Procedures." *B*, to precisely quantify results, the $TREX1^{WT}$ and variant enzymes were assayed in triplicate at three different concentrations as described above. $TREX1^{WT}$ was assayed at 8, 15, and 20 pM, $TREX1^{WT/R114A}$, $TREX1^{WT/R114K}$, $TREX1^{R114A/A124ins}$, and $TREX1^{R114K/A124ins}$ were assayed at 30, 45, and 60 pM, and $TREX1^{R114A/R114A}$ and $TREX1^{R114K/R114K}$ were assayed at 100, 150, and 200 pM. Plots of activity *versus* enzyme concentrations were used to confirm the linearity of the assay and generate the enzyme activity values. The average activities and S.E. were determined by regression analysis using SigmaPlot 8.02 (SPSS Science, Inc.). The relative activity was calculated as: relative activity = 100 × ((femtomole of dNMP released/s/fmol of mutant enzyme)/(fmol of dNMP released/s/fmol of WT enzyme)). The position of migration of the 30-mer is indicated.

erodimers. It is likely that the R114H mutation results in destabilization of the flexible loop between the α3 and α4 helices in the opposing protomer preventing the α2 helix from appropriately interacting with the nitrogenous base of the incoming 3′ nucleotide. Thus, the effect of the R114H mutation is transferred to the active site of the opposing protomer in the TREX1 dimer.

Arg-114 Is Required for Full Activity in the TREX1 Dimer—Arg-114 in TREX1 (Arg-107 in TREX2) is conserved in the mammalian dimeric 3′ exonucleases (19, 20). TREX1 mutants R114A and R114K were generated to further test the requirement for arginine at this position. The R114A mutation eliminates the positively charged arginine side chain and replaces it with the short neutral side chain of alanine. This amino acid substitution was used to determine whether the loss of catalytic activity in the $TREX1^{R114H}$ could be attributed to the loss of the arginine or to the presence of histidine at this position. The R114K mutation was prepared to determine whether the long, basic side chain of lysine could substitute for arginine at this position. The ssDNA degradation activities of the $TREX1^{R114A}$ and $TREX1^{R114K}$ homodimers are reduced by 22- and 11-fold, respectively, compared with $TREX1^{WT}$ (Fig. 4). The similarly reduced activities of $TREX1^{R114H}$ and $TREX1^{R114A}$ homodimers compared with $TREX1^{WT}$ indicate that it is the loss of arginine at this position that contributes mostly to the reduced catalytic function. This conclusion is further supported by the 11-fold reduced ssDNA degradation activity detected in the $TREX1^{R114K}$ homodimer compared with $TREX1^{WT}$. This rather dramatic loss of catalytic function is detected despite the relatively conserved substitution of lysine for arginine at position 114. Together, the loss of ssDNA exonuclease activities in these Arg-114 mutations demonstrates the requirement for arginine at position 114 in TREX1.

The R114A and R114K Mutations Contribute to Reduced ssDNA Exonuclease Activity in the Opposing TREX1 Protomer—The $TREX1^{WT/R114A}$, $TREX1^{R114A/A124ins}$, $TREX1^{WT/R114K}$, and $TREX1^{R114K/A124ins}$ heterodimers were prepared and the ssDNA exonuclease activities were measured (Fig. 4). The $TREX1^{WT/R114A}$ heterodimer exhibits ssDNA exonuclease activity 1/3.8 of that measured for the $TREX1^{WT}$ enzyme. The activity of the $TREX1^{R114A/A124ins}$ compound heterodimer is 1/5.8 of $TREX1^{WT}$. Similar ssDNA exonuclease activities in $TREX1^{WT/R114A}$ and $TREX1^{R114A/A124ins}$ heterodimers support the concept that mutations in TREX1 at Arg-114 predominantly affect activity in the opposing protomer of the TREX1 dimer and contribute less to activity in the TREX1 protomer containing the Arg-114 mutation. Similarly, the $TREX1^{WT/R114K}$ heterodimer exhibits ssDNA exonuclease activity 1/2.5 of that measured for the $TREX1^{WT}$ enzyme. The activity of the $TREX1^{R114K/A124ins}$ compound heterodimer is 1/3.2 of $TREX1^{WT}$. The $TREX1^{WT/R114K}$ and $TREX1^{R114K/A124ins}$ heterodimers exhibit ssDNA degradation activities greater than

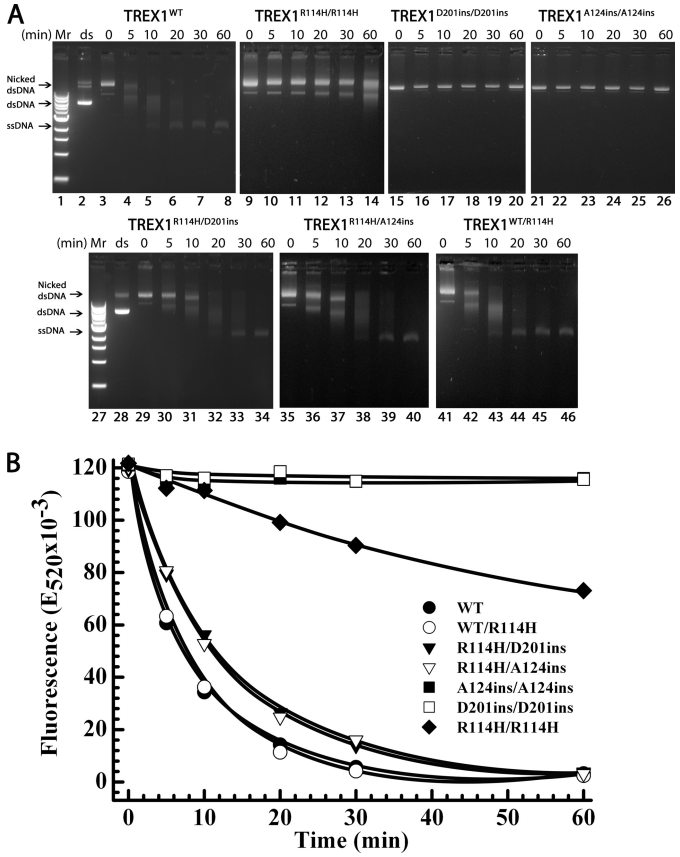

FIGURE 5. **The dsDNA degradation activities of TREX1 R114H-containing mutants.** The supercoiled dsDNA plasmid 1 (*A*, *lanes 2* and *28*) was nicked and purified as described under "Experimental Procedures." Exonuclease time course reactions (200 μl) were prepared containing nicked dsDNA plasmid 1 (10 μg/ml) and 15 nM of the indicated TREX1 enzyme. Samples (20 μl) were removed after incubation for the indicated times and subjected to electrophoresis on agarose gels (*A*) or quenched in 20 μl of 15× aqueous SYBR Green I dye (*B*) (Invitrogen). The positions of migration of Form I supercoiled dsDNA (*dsDNA*), Form II nicked dsDNA (*Nicked dsDNA*), and circular ssDNA (*ssDNA*) are indicated. *Lanes 1* and *27* contain the 1-kb ladder (Invitrogen). The SYBR Green-quenched reaction products were quantified by excitation at 480 nM and emission was measured at 520 nM. The plot of fluorescence ($E_{520} \times 10^{-3}$) *versus* time was generated using SigmaPlot 8.02 (SPSS Science, Inc.).

TABLE 1
The dsDNA exonuclease activity of TREX1^{WT} and variants

TREX1	dsDNA activity[a]	Relative activity[b]
	fmol/s/fmol E	
WT	8.2 ± 0.31	1
R114H/R114H	0.34 ± 0.028	1/24
D201ins/D201ins	ND[c]	ND
A124ins/A124ins	ND	ND
R114H/D201ins	3.9 ± 0.20	1/2.1
R114H/A124ins	3.5 ± 0.33	1/2.6
R114H/WT	5.2 ± 0.49	1/1.6
R114A/R114A	0.45 ± 0.038	1/18
R114K/R114K	0.93 ± 0.051	1/8.8
R114A/A124ins	1.1 ± 0.01	1/7.6
R114K/A124ins	3.2 ± 0.38	1/2.6
R114A/WT	2.0 ± 0.21	1/4.2
R114K/WT	3.2 ± 0.12	1/2.6

[a] Exonuclease reactions (200 μl) were prepared containing nicked dsDNA plasmid 1 (10 μg/ml) and TREX1^{WT} at 0.5, 1.0, and 1.5 nM, TREX1$^{R114H/R114H}$ and TREX1$^{R114A/R114A}$ at 40, 60, and 80 nM, TREX1$^{R114K/R114K}$ at 10, 15, and 20 nM, TREX1$^{WT/R114H}$, TREX1$^{R114H/D201ins}$, TREX1$^{R114H/A124ins}$, TREX1$^{WT/R114K}$, and TREX1$^{R114K/A124ins}$ at 1, 1.5, and 2 nM, and TREX1$^{WT/R114A}$ and TREX1$^{R114A/A124ins}$ at 2, 3, and 4 nM. Samples were removed at 10, 15, 20, 25, and 30 min and dsDNA degradation was quantified as described under "Experimental Procedures." Plots of activity *versus* enzyme concentrations confirmed linearity of the assay and were used to generate the enzyme activity values. The average activities and standard errors were determined by regression analysis using SigmaPlot 8.02 (SPSS Science, Inc.).

[b] The relative activity was calculated as: relative activity = 100 × ((femtomole of dNMP released/s/fmol of mutant enzyme)/(fmol of dNMP released/s/fmol of WT enzyme)).

[c] ND, not determined.

that of the TREX1^{R114K} homodimer (Fig. 4). Thus, the TREX1^{A124ins} protomer contributes to exonuclease activity in the TREX1$^{R114K/A124ins}$ heterodimer just as the TREX1^{WT} protomer contributes to activity in the TREX1$^{R114K/WT}$ heterodimer despite the nearly complete loss of catalytic activity in the TREX1^{A124ins} protomer. These data further indicate that TREX1 Arg-114 of one protomer contributes to the ssDNA exonuclease activity in the opposing protomer.

The TREX1 3′ dsDNA Exonuclease Activities of R114H-containing Mutants—Arg-114 in the TREX1^{D201ins} and TREX1^{A124ins} protomers contributes to dsDNA exonuclease activities of the TREX1^{R114H} protomer in the TREX1$^{R114H/D201ins}$ and TREX1$^{R114H/A124ins}$ compound heterodimers. The dsDNA degradation activities of the R114H-containing mutants were directly compared in time course reactions using a nicked DNA plasmid (Fig. 5). The products were visualized on agarose gels (Fig. 5*A*) and quantified using SYBR Green fluorescence (Fig. 5*B*). Incubation of the nicked DNA with TREX1^{WT} results in >97% complete degradation of the nicked polynucleotide strand and the accumulation of the un-nicked ssDNA (Fig. 5*A*, *lanes 3–8*). The TREX1$^{R114H/R114H}$ homodimer degrades the nicked DNA less efficiently compared with TREX1^{WT} with ~40% of the nicked DNA degraded and no detectible accumulation of the ssDNA (Fig. 5*A*, *lanes 9–14*). The TREX1$^{D201ins/D201ins}$ (Fig. 5*A*, *lanes 15–20*) and TREX1$^{A124ins/A124ins}$ (Fig. 5*A*, *lanes 21–26*) exhibit no detectable dsDNA degradation activity. However, the TREX1$^{R114H/D201ins}$ (Fig. 5*A*, *lanes 29–34*) and TREX1$^{R114H/A124ins}$ (Fig. 5*A*, *lanes 35–40*) compound heterodimers exhibit dramatically higher dsDNA degradation activities compared with the TREX1$^{R114H/R114H}$ homodimer with obvious accumulation of the unnicked ssDNA. The activities of the TREX1$^{R114H/D201ins}$ and TREX1$^{R114H/A124ins}$ compound heterodimers are similar to the TREX1$^{WT/R114H}$ (Fig. 5*A*, *lanes 41–46*). Thus, despite the lack of dsDNA degradation activities in the TREX1^{D201ins} and TREX1^{A124ins} protomers, these mutant protomers contribute to dsDNA degradation activity in the TREX1 R114H-containing dimer nearly as well as the TREX1^{WT} protomer.

The dsDNA degradation activities of the TREX1 R114H-containing enzymes were precisely quantified using the nicked plasmid DNA (Table 1). The dsDNA exonuclease activity of the TREX1$^{R114H/R114H}$ homodimer is reduced 24-fold compared with TREX1^{WT} and the TREX1$^{D201ins/D201ins}$ and TREX1$^{A124ins/A124ins}$ homodimers exhibit no detectable activity. The TREX1$^{R114H/D201ins}$, TREX1$^{R114H/A124ins}$, and TREX1$^{WT/R114H}$ heterodimers exhibit reduced activities of 2.1-, 2.6-, and 1.6-fold, respectively, compared with TREX1^{WT} (Table 1). Thus, the TREX1$^{R114H/D201ins}$ and TREX1$^{R114H/A124ins}$ compound heterodimers are ~20-fold more active than would be expected based on the dsDNA activities of the TREX1$^{D201ins/D201ins}$ and TREX1$^{A124ins/A124ins}$ homodimers. These dramatically higher heterodimer activities parallel the higher than expected activities for ssDNA degradation by these same enzymes.

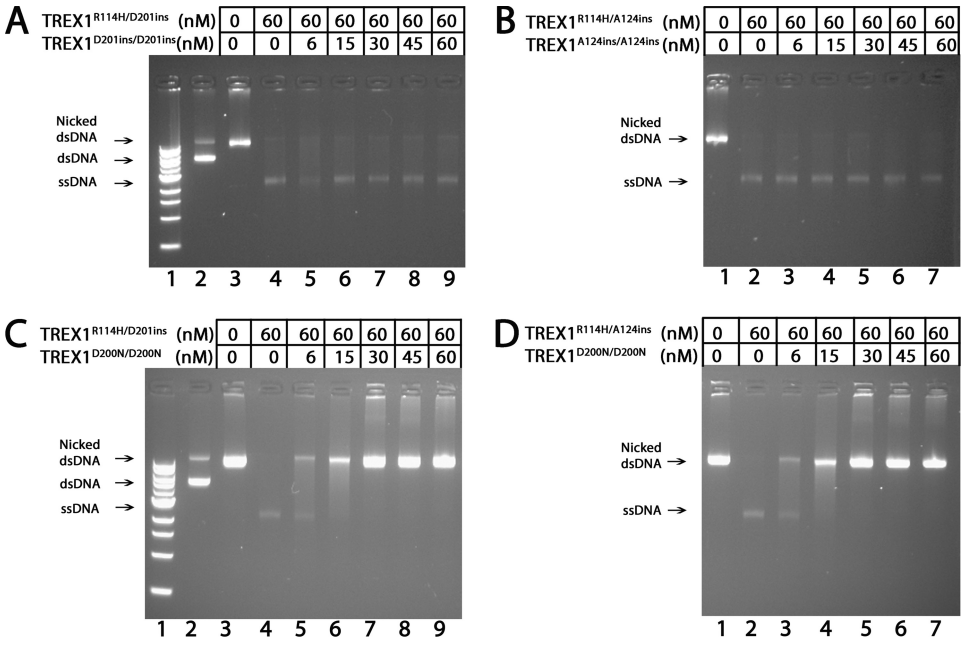

FIGURE 6. **The TREX1^{D201ins} and TREX1^{A124ins} mutants are recessive to TREX1^{R114H} compound heterodimer dsDNA degradation.** The supercoiled dsDNA plasmid 1 (*A* and *C*, *lane 2*) was nicked and purified as described under "Experimental Procedures." Exonuclease reactions (20 μl) were prepared containing nicked dsDNA plasmid 1 (10 μg/ml) and no enzyme (*A* and *C*, *lane 3*; and *B* and *D*, *lane 1*), or 60 nM TREX1$^{R114H/D201ins}$ (*A* and *C*, *lanes 4–9*) or TREX1$^{R114H/A124ins}$ (*B* and *D*, *lanes 2–7*), and the indicated concentrations of TREX1$^{D201ins/D201ins}$ (*A*, *lanes 5–9*), TREX1$^{A124ins/A124ins}$ (*B*, *lanes 3–7*), or TREX1$^{D200N/D200N}$ (*C*, *lanes 5–9*; and *D*, *lanes 3–7*). The reactions were incubated 60 min at 25 °C, and the products were separated by electrophoresis on agarose gels stained with ethidium bromide. The positions of migration of Form I supercoiled dsDNA (*dsDNA*), Form II nicked dsDNA (*Nicked dsDNA*), and circular ssDNA (*ssDNA*) are indicated. *Lane 1* (*A* and *B*) contains the 1-kb ladder (Invitrogen).

The TREX1 3′ dsDNA Exonuclease Activities of R114A- and R114K-containing Mutants—The dsDNA exonuclease activities of the TREX1 R114A- and R114K-containing mutants were measured (Table 1). The TREX1$^{R114A/R114A}$ activity is 18-fold lower than TREX1^{WT} and TREX1$^{R114K/R114K}$ is reduced 8.8-fold. The TREX1$^{R114A/A124ins}$ and TREX1$^{R114K/A124ins}$ compound heterodimers are 7.6- and 2.6-fold reduced relative to TREX1^{WT}. The TREX1$^{R114A/WT}$ and TREX1$^{R114K/WT}$ heterodimers exhibit a 4.2- and 2.6-fold reduced activity compared with TREX1^{WT} (Table 1). Thus, the activities of the TREX1$^{R114A/A124ins}$ and TREX1$^{R114K/A124ins}$ heterodimers are about 5- and 7-fold more active than would be expected from the dsDNA degradation activities of their respective homodimers. The dsDNA degradation activities measured in the TREX1 Arg-114 containing mutants support the concept that Arg-114 contributes to the catalytic activity in the active site of the opposing protomer during dsDNA degradation.

The TREX1^{D201ins} and TREX1^{A124ins} Mutants Are Recessive to TREX1^{R114H} Compound Heterodimer dsDNA Degradation—The TREX1 D201ins and A124ins mutations have been identified as homozygous and as compound heterozygous mutations with R114H in recessive AGS (8, 9). An AGS-affected individual with the *TREX1*$^{R114H/D201ins}$ or *TREX1*$^{R114H/A124ins}$ genotype could generate TREX1 dimers as mixtures of TREX1$^{R114H/R114H}$, TREX1$^{R114H/(D201ins\ or\ A124ins)}$, and TREX1$^{D201ins/D201ins}$ or TREX1$^{A124ins/A124ins}$. The TREX1$^{R114H/D201ins}$ and TREX1$^{R114H/A124ins}$ dsDNA degradation activities were measured in the presence of increasing amounts of the TREX1$^{D201ins/D201ins}$ and TREX1$^{A124ins/A124ins}$ homodimers to measure possible inhibitory effects on the compound heterodimers. Incubation of the nicked plasmid DNA with 60 nM TREX1$^{R114H/D201ins}$ (Fig. 6*A, lane 4*) and TREX1$^{R114H/A124ins}$ (Fig. 6*B, lane 2*) results in complete degradation of the nicked DNA as evidenced by the accumulation of the unnicked ssDNA. Similarly, upon addition of increased amounts of the TREX1$^{D201ins/D201ins}$ (Fig. 6*A, lanes 5–9*) or TREX1$^{A124ins/A124ins}$ (Fig. 6*B, lanes 3–7*), TREX1$^{R114H/D201ins}$ and TREX1$^{R114H/A124ins}$ completely degrade the nicked DNA indicating the lack of inhibition by these enzymes. These results contrast with the complete inhibition of dsDNA degradation by TREX1$^{R114H/D201ins}$ (Fig. 6*C, lane 4*) and TREX1$^{R114H/A124ins}$ (Fig. 6*D, lane 2*) upon addition of increased amounts of the TREX1$^{D200N/D200N}$ (Fig. 6, *C, lanes 5–9,* and *D, lanes 3–7*). These results are consistent with the recessive genetics of the *TREX1* D201ins and A124ins alleles.

The Stable TREX1 Dimer—The strength of the TREX1 dimer has implications for the enzymatic behavior during DNA degradation to prevent nucleic acid-mediated immune activation. The TREX1 dimeric structure is conserved in all species expressing this enzyme indicating that the dimeric architecture is critical for its biologic and enzymatic functions. TREX1 protomers interact in the dimer along the outermost β3-strands forming an extended central antiparallel β-sheet that stretches through the length of the dimer. The remarkable strength of the TREX1 dimer indicated in structural studies (20) is validated here in solution studies demonstrating that TREX1 does not dissociate and re-equilibrate at measurable rates after the dimer is generated when expressed in bacterial cells. It is likely that TREX1 dimers exhibit similar stability properties when expressed in mammalian cells. This concept is supported by the dominant disease genetics exhibited by some *TREX1* alleles that parallel precisely the biochemical properties

of the TREX1 dimers during dsDNA degradation of plasmid and chromatin DNA *in vitro* (23, 26). Our finding that Arg-114 in one protomer contributes to the catalytic function in the active site of the opposing protomer provides the first direct evidence for a required TREX1 dimeric structure for full catalytic competency. This "across the dimer interface" action by Arg-114 might help to explain the immune dysfunction in some R114H heterozygous cases (13, 14). In addition, many TREX1 mutations in lupus and retinal vasculopathy with cerebral leukodystrophy (12) are heterozygous and locate outside the catalytic domain in the C-terminal region. The stable TREX1 dimeric structure could lead to dominant noncatalytic dysfunction effects related to cellular localization or protein interactions.

Acknowledgment—We thank Y. Crow for providing unpublished data on TREX1 AGS-causing alleles.

REFERENCES

1. Höss, M., Robins, P., Naven, T. J., Pappin, D. J., Sgouros, J., and Lindahl, T. (1999) *EMBO J.* **18,** 3868–3875
2. Mazur, D. J., and Perrino, F. W. (1999) *J. Biol. Chem.* **274,** 19655–19660
3. Mazur, D. J., and Perrino, F. W. (2001) *J. Biol. Chem.* **276,** 17022–17029
4. Mazur, D. J., and Perrino, F. W. (2001) *J. Biol. Chem.* **276,** 14718–14727
5. Morita, M., Stamp, G., Robins, P., Dulic, A., Rosewell, I., Hrivnak, G., Daly, G., Lindahl, T., and Barnes, D. E. (2004) *Mol. Cell. Biol.* **24,** 6719–6727
6. Stetson, D. B., Ko, J. S., Heidmann, T., and Medzhitov, R. (2008) *Cell* **134,** 587–598
7. Yang, Y. G., Lindahl, T., and Barnes, D. E. (2007) *Cell* **131,** 873–886
8. Crow, Y. J., Hayward, B. E., Parmar, R., Robins, P., Leitch, A., Ali, M., Black, D. N., van Bokhoven, H., Brunner, H. G., Hamel, B. C., Corry, P. C., Cowan, F. M., Frints, S. G., Klepper, J., Livingston, J. H., Lynch, S. A., Massey, R. F., Meritet, J. F., Michaud, J. L., Ponsot, G., Voit, T., Lebon, P., Bonthron, D. T., Jackson, A. P., Barnes, D. E., and Lindahl, T. (2006) *Nat. Genet.* **38,** 917–920
9. Rice, G., Patrick, T., Parmar, R., Taylor, C. F., Aeby, A., Aicardi, J., Artuch, R., Montalto, S. A., Bacino, C. A., Barroso, B., Baxter, P., Benko, W. S., Bergmann, C., Bertini, E., Biancheri, R., Blair, E. M., Blau, N., Bonthron, D. T., Briggs, T., Brueton, L. A., Brunner, H. G., Burke, C. J., Carr, I. M., Carvalho, D. R., Chandler, K. E., Christen, H. J., Corry, P. C., Cowan, F. M., Cox, H., D'Arrigo, S., Dean, J., De Laet, C., De Praeter, C., Dery, C., Ferrie, C. D., Flintoff, K., Frints, S. G., Garcia-Cazorla, A., Gener, B., Goizet, C., Goutieres, F., Green, A. J., Guet, A., Hamel, B. C., Hayward, B. E., Heiberg, A., Hennekam, R. C., Husson, M., Jackson, A. P., Jayatunga, R., Jiang, Y. H., Kant, S. G., Kao, A., King, M. D., Kingston, H. M., Klepper, J., van der Knaap, M. S., Kornberg, A. J., Kotzot, D., Kratzer, W., Lacombe, D., Lagae, L., Landrieu, P. G., Lanzi, G., Leitch, A., Lim, M. J., Livingston, J. H., Lourenco, C. M., Lyall, E. G., Lynch, S. A., Lyons, M. J., Marom, D., McClure, J. P., McWilliam, R., Melancon, S. B., Mewasingh, L. D., Moutard, M. L., Nischal, K. K., Ostergaard, J. R., Prendiville, J., Rasmussen, M., Rogers, R. C., Roland, D., Rosser, E. M., Rostasy, K., Roubertie, A., Sanchis, A., Schiffmann, R., Scholl-Burgi, S., Seal, S., Shalev, S. A., Corcoles, C. S., Sinha, G. P., Soler, D., Spiegel, R., Stephenson, J. B., Tacke, U., Tan, T. Y., Till, M., Tolmie, J. L., Tomlin, P., Vagnarelli, F., Valente, E. M., Van Coster, R. N., Van der Aa, N., Vanderver, A., Vles, J. S., Voit, T., Wassmer, E., Weschke, B., Whiteford, M. L., Willemsen, M. A., Zankl, A., Zuberi, S. M., Orcesi, S., Fazzi, E., Lebon, P., and Crow, Y. J. (2007) *Am. J. Hum. Genet.* **81,** 713–725
10. Lee-Kirsch, M. A., Chowdhury, D., Harvey, S., Gong, M., Senenko, L., Engel, K., Pfeiffer, C., Hollis, T., Gahr, M., Perrino, F. W., Lieberman, J., and Hubner, N. (2007) *J. Mol. Med.* **85,** 531–537
11. Rice, G., Newman, W. G., Dean, J., Patrick, T., Parmar, R., Flintoff, K., Robins, P., Harvey, S., Hollis, T., O'Hara, A., Herrick, A. L., Bowden, A. P., Perrino, F. W., Lindahl, T., Barnes, D. E., and Crow, Y. J. (2007) *Am. J. Hum. Genet.* **80,** 811–815
12. Richards, A., van den Maagdenberg, A. M., Jen, J. C., Kavanagh, D., Bertram, P., Spitzer, D., Liszewski, M. K., Barilla-Labarca, M. L., Terwindt, G. M., Kasai, Y., McLellan, M., Grand, M. G., Vanmolkot, K. R., de Vries, B., Wan, J., Kane, M. J., Mamsa, H., Schäfer, R., Stam, A. H., Haan, J., de Jong, P. T., Storimans, C. W., van Schooneveld, M. J., Oosterhuis, J. A., Gschwendter, A., Dichgans, M., Kotschet, K. E., Hodgkinson, S., Hardy, T. A., Delatycki, M. B., Hajj-Ali, R. A., Kothari, P. H., Nelson, S. F., Frants, R. R., Baloh, R. W., Ferrari, M. D., and Atkinson, J. P. (2007) *Nat. Genet.* **39,** 1068–1070
13. Lee-Kirsch, M. A., Gong, M., Chowdhury, D., Senenko, L., Engel, K., Lee, Y. A., de Silva, U., Bailey, S. L., Witte, T., Vyse, T. J., Kere, J., Pfeiffer, C., Harvey, S., Wong, A., Koskenmies, S., Hummel, O., Rohde, K., Schmidt, R. E., Dominiczak, A. F., Gahr, M., Hollis, T., Perrino, F. W., Lieberman, J., and Hübner, N. (2007) *Nat. Genet.* **39,** 1065–1067
14. Namjou, B., Kothari, P. H., Kelly, J. A., Glenn, S. B., Ojwang, J. O., Adler, A., Alarcón-Riquelme, M. E., Gallant, C. J., Boackle, S. A., Criswell, L. A., Kimberly, R. P., Brown, E., Edberg, J., Stevens, A. M., Jacob, C. O., Tsao, B. P., Gilkeson, G. S., Kamen, D. L., Merrill, J. T., Petri, M., Goldman, R. R., Vila, L. M., Anaya, J. M., Niewold, T. B., Martin, J., Pons-Estel, B. A., Sabio, J. M., Callejas, J. L., Vyse, T. J., Bae, S. C., Perrino, F. W., Freedman, B. I., Scofield, R. H., Moser, K. L., Gaffney, P. M., James, J. A., Langefeld, C. D., Kaufman, K. M., Harley, J. B., and Atkinson, J. P. (2011) *Genes Immun.* **12,** 270–279
15. Kavanagh, D., Spitzer, D., Kothari, P. H., Shaikh, A., Liszewski, M. K., Richards, A., and Atkinson, J. P. (2008) *Cell Cycle* **7,** 1718–1725
16. Kolivras, A., Aeby, A., Crow, Y. J., Rice, G. I., Sass, U., and André, J. (2008) *J. Cutan. Pathol.* **35,** 774–778
17. Crow, Y. J., and Rehwinkel, J. (2009) *Hum. Mol. Genet.* **18,** R130–136
18. Ramantani, G., Kohlhase, J., Hertzberg, C., Innes, A. M., Engel, K., Hunger, S., Borozdin, W., Mah, J. K., Ungerath, K., Walkenhorst, H., Richardt, H. H., Buckard, J., Bevot, A., Siegel, C., von Stülpnagel, C., Ikonomidou, C., Thomas, K., Proud, V., Niemann, F., Wieczorek, D., Häusler, M., Niggemann, P., Baltaci, V., Conrad, K., Lebon, P., and Lee-Kirsch, M. A. (2010) *Arthritis Rheum.* **62,** 1469–1477
19. Perrino, F. W., Harvey, S., McMillin, S., and Hollis, T. (2005) *J. Biol. Chem.* **280,** 15212–15218
20. de Silva, U., Choudhury, S., Bailey, S. L., Harvey, S., Perrino, F. W., and Hollis, T. (2007) *J. Biol. Chem.* **282,** 10537–10543
21. Parra, D., Manils, J., Castellana, B., Viña-Vilaseca, A., Morán-Salvador, E., Vázquez-Villoldo, N., Tarancón, G., Borràs, M., Sancho, S., Benito, C., Ortega, S., and Soler, C. (2009) *Cancer Res.* **69,** 6676–6684
22. Chowdhury, D., Beresford, P. J., Zhu, P., Zhang, D., Sung, J. S., Demple, B., Perrino, F. W., and Lieberman, J. (2006) *Mol. Cell* **23,** 133–142
23. Lehtinen, D. A., Harvey, S., Mulcahy, M. J., Hollis, T., and Perrino, F. W. (2008) *J. Biol. Chem.* **283,** 31649–31656
24. Günther, C., Meurer, M., Stein, A., Viehweg, A., and Lee-Kirsch, M. A. (2009) *Dermatology* **219,** 162–166
25. Haaxma, C. A., Crow, Y. J., van Steensel, M. A., Lammens, M. M., Rice, G. I., Verbeek, M. M., and Willemsen, M. A. (2010) *Am. J. Med. Genet. A* **152A,** 2612–2617
26. Fye, J. M., Orebaugh, C. D., Coffin, S. R., Hollis, T., and Perrino, F. W. (2011) *J. Biol. Chem.* **286,** 32373–32382
27. Higuchi, R. (1990) *PCR Protocols: A Guide to Methods and Applications*, Academic Press, San Diego
28. Perrino, F. W., Miller, H., and Ealey, K. A. (1994) *J. Biol. Chem.* **269,** 16357–16363